

## High-Energy Spin Dynamics in $\text{La}_{1.69}\text{Sr}_{0.31}\text{NiO}_4$

P. Bourges,<sup>1</sup> Y. Sidis,<sup>1</sup> M. Braden,<sup>1,2,\*</sup> K. Nakajima,<sup>3</sup> and J. M. Tranquada<sup>4</sup>

<sup>1</sup>Laboratoire Léon Brillouin, CEA-CNRS, CE-Saclay, 91191 Gif sur Yvette, France

<sup>2</sup>Forschungszentrum Karlsruhe, IFP, Postfach 3640, D-76021 Karlsruhe, Germany

<sup>3</sup>Neutron Scattering Laboratory, ISSP, University of Tokyo, Tokai, Ibaraki, Japan

<sup>4</sup>Physics Department, Brookhaven National Laboratory, Upton, New York 11973

(Received 8 March 2002; published 9 April 2003)

To test the prediction that the dispersion of the magnetic resonance in superconducting  $\text{YBa}_2\text{Cu}_3\text{O}_{6+x}$  is similar to magnons in an incommensurate antiferromagnet, we have mapped out the spin dynamics in a stripe-ordered nickelate,  $\text{La}_{2-x}\text{Sr}_x\text{NiO}_4$ , with  $x \approx 0.31$ , using inelastic neutron scattering. We observe spin-wave excitations up to 80 meV emerging from the incommensurate magnetic peaks with a surprisingly large and almost isotropic spin velocity:  $\hbar c_s \sim 0.32 \text{ eV \AA}$ . A comparison indicates that the inferred spin-excitation spectrum is not, by itself, an adequate model for the magnetic resonance feature of the superconductor.

DOI: 10.1103/PhysRevLett.90.147202

PACS numbers: 75.30.Ds, 25.40.Fq, 64.70.Rh

Magnetism plays an important role in several theories of the high-temperature superconductivity found in layered cuprates. Much attention has been focused on the “resonance” peak observed by inelastic neutron scattering in a number of different cuprates [1]. The resonance peak is centered commensurately on the antiferromagnetic wave vector. Studies of  $\text{YBa}_2\text{Cu}_3\text{O}_{6+x}$ , in which the resonance peak was first observed [2], have also found incommensurate excitations at somewhat lower energies [3,4]. In a recent paper [5], it was found that the incommensurate scattering actually disperses downward continuously from the commensurate resonance peak, apparently defining a single dispersive excitation.

In one popular approach, the magnetic resonance is understood as a particle-hole bound state below the two-particle continuum associated with the  $d$ -wave superconducting gap [6–9]; such calculations, based on a homogeneous, renormalized Fermi-liquid model, yield qualitative agreement with experiment. One alternative is based on the “stripe” scenario [10,11], in which magnetic excitations are dominantly attributed to spatially segregated domains of antiferromagnetically correlated copper spins [12–16]. In particular, Batista, Ortiz, and Balatsky [17] have explicitly proposed that the dispersive resonance represents the magnonlike excitations emanating from incommensurate wave vectors associated with a stripe-correlated spin system. Their prediction that a similar resonance-like excitation should be observable in a stripe-ordered compound such as  $\text{La}_{2-x}\text{Sr}_x\text{NiO}_4$  motivated the present investigation.

Regardless of whether  $\text{La}_{2-x}\text{Sr}_x\text{NiO}_4$  is an ideal model for the cuprates, studies of the full spin dynamics of the incommensurate spin state are of interest, as only low-energy characterizations have been reported previously [18,19]. Here we report measurements of the high-energy spin excitations in a crystal with  $x \approx 0.31$ , close to the 1/3 composition. Within the two-dimensional reciprocal space corresponding to a doped  $\text{NiO}_2$  plane, the diagonal

stripe order yields two pairs of magnetic ordering wave vectors,  $\mathbf{Q}_\delta = (\frac{1}{2}, \frac{1}{2}) \pm (\delta, \delta)$  and  $(\frac{1}{2}, \frac{1}{2}) \pm (\delta, -\delta)$ , due to twinning of the stripe domains. [We express wave vectors in units of the reciprocal lattice,  $(2\pi/a, 2\pi/a)$ , with  $a = 3.82 \text{ \AA}$ .] These incommensurate points are displaced about the antiferromagnetic propagation wave vector,  $\mathbf{Q}_{\text{AF}} = (\frac{1}{2}, \frac{1}{2})$ , of the undoped parent compound. The incommensurability  $\delta$  varies with the hole concentration as  $\delta \approx x/2$  [20], with  $\delta = 0.158$  for our sample at low temperature. We observed spin-wave excitations dispersing from each  $\mathbf{Q}_\delta$  peak up to a maximum of 80 meV at  $\mathbf{Q}_{\text{AF}}$ , which resemble those expected for an incommensurate antiferromagnet. On warming to above the charge-ordering temperature, the excitation at  $\mathbf{Q}_{\text{AF}}$  softens somewhat, but remains well-defined. A comparison of the relevant features indicates substantial differences from the resonance observed in  $\text{YBa}_2\text{Cu}_3\text{O}_{6.85}$  [5].

Our single-crystal sample, grown by the floating-zone method, was the subject of a previous neutron scattering experiment [21]. The present inelastic-neutron-scattering measurements were performed on the 1T and 2T triple-axis spectrometers at the Orphée reactor of the Laboratoire Léon Brillouin in Saclay, France. Each spectrometer is equipped with Cu(111) and pyrolytic graphite (PG) monochromators and a PG (002) analyzer. Different final neutron energies of the analyzer,  $E_f = 14.7, 30.5,$  and  $41 \text{ meV}$ , were used as necessary in order to cover the full energy range of the magnetic spectrum. A PG filter was placed after the sample to minimize neutrons at higher-harmonic wavelengths. Most of the measurements have been performed within the  $(HK0)$  scattering plane, with some data collected in the  $(HHL)$  zone.

In scanning across the  $\mathbf{Q}_\delta$  peak positions at constant-energy transfer, as indicated in the upper panel of Fig. 1, we expect, at low temperatures (below the spin-ordering temperature of 160 K), to pass through two spin-wave branches, corresponding to counterpropagating excitations. The lower panels show scans at an energy transfer

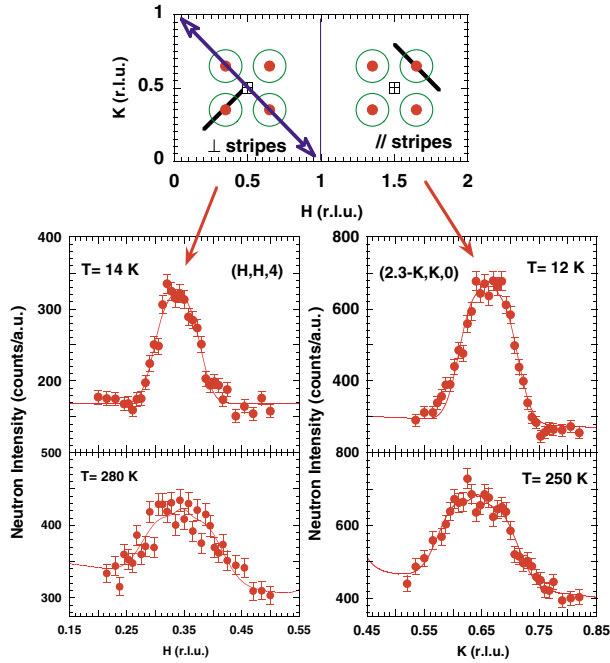


FIG. 1 (color online). Upper panel: Sketch of the Brillouin zone in the reciprocal  $(HK0)$  plane. Full circles indicate the location of the incommensurate magnetic peaks,  $\mathbf{Q}_\delta$ . The circles (around  $\mathbf{Q}_\delta$ ) show the cut of the spin-wave cones at a constant energy, defining  $Q_\omega$  ( $\equiv \omega/c_s$  in the low-energy regime). Full bars represent the directions of the scans shown in the lower panel; the arrow shows the direction of the scans shown in Fig. 2. Lower panels: Constant energy scans at  $E = 28.1$  meV (measured with  $E_f = 14.7$  meV) at two temperatures along the two directions sketched in the upper panel, probing fluctuations along wave vectors perpendicular (left) and parallel (right) to the stripes. Lines represent best fits of the extended Gaussian model described in the text.

of 28.1 meV along orthogonal directions with respect to the modulation wave vector. Although the two branches are not resolved, the  $Q$  width in each case is significantly broader than resolution, with little dependence on scan direction. At higher energies [Fig. 2(b)–2(d)], the data are clearly consistent with spin waves emerging from the two  $\mathbf{Q}_\delta$  points  $(1.5 - \delta, 1.5 + \delta)$  and  $(1.5 + \delta, 1.5 - \delta)$ . At  $E = 75$  meV, the excitations from  $+\delta$  and  $-\delta$  begin to merge at  $\mathbf{Q}_{AF}$ , forming a single broad peak, with additional weight coming from excitations associated with the orthogonal stripe domains (see Fig. 1).

The excitation at  $\mathbf{Q}_{AF}$  is better characterized by scanning the energy transfer at fixed momentum transfer. Figure 3(b)–3(d) shows energy scans at  $\mathbf{Q}_{AF}$  for three different temperatures. The maximum of the spin-excitation spectrum is  $\omega_0 = 80 \pm 0.8$  meV at low temperature [Fig. 3(b)].

In the studies of low-energy excitations in stripe-correlated nickelates [18,19], it was found that the observed  $Q$  widths of the excitation peaks are broader than the energy resolution. For Sr-doped samples, this is due, at least in part, to the finite spin-spin correlation length

in the ordered state. Fluctuations of the charge stripes might also play a role. To extract the frequency dispersion from the constant-energy scans of Figs. 1 and 2, we have assumed a scattering function of the form

$$S(\mathbf{Q}, \omega) = Af^2(Q) \sum_{\text{domains}} \sum_{\delta} e^{-[(\mathbf{Q}-\mathbf{Q}_\delta)^2 - \mathbf{Q}_\omega^2]/2\Delta^2}, \quad (1)$$

where  $A$  is a scale factor, one sum is over the two incommensurate wave vectors, the other one is over the twined

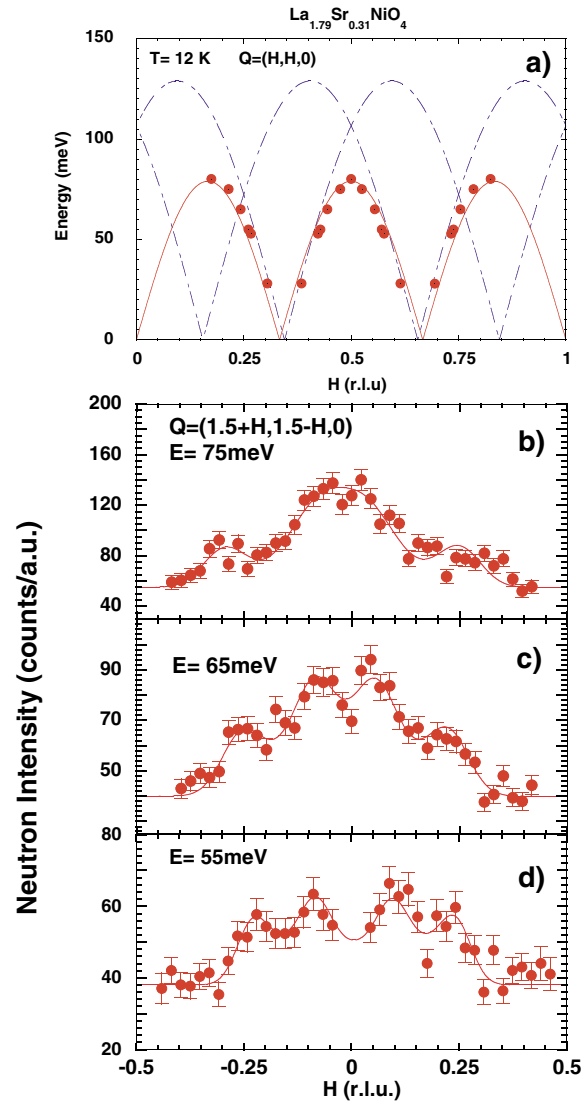


FIG. 2 (color online). (a) Dispersion relation of the spin excitations in  $\text{La}_{1.69}\text{Sr}_{0.31}\text{NiO}_4$ . The solid line is a fit by a simple  $|\sin(3\pi H)|$  function. The two dashed lines correspond to the spin-wave dispersion relation in undoped  $\text{La}_2\text{NiO}_4$ , but shifted to the incommensurate wave vectors. (b)–(d) Constant energy scans at (b)  $E = 75$  meV, (c)  $E = 65$  meV, and (d)  $E = 55$  meV along  $(H, -H, 0)$  (i.e., perpendicular to the stripes) around  $Q = (1.5, 1.5, 0)$ . Scan (b) was measured with  $E_f = 41$  meV (as in Fig. 3), while (c) and (d) were measured with  $E_f = 30.5$  meV. The error bars reflect a total counting time of 15 min/point in (b) and 10 min/point in (c)–(d). Full lines represent best fits of the extended Gaussian model described in the text.

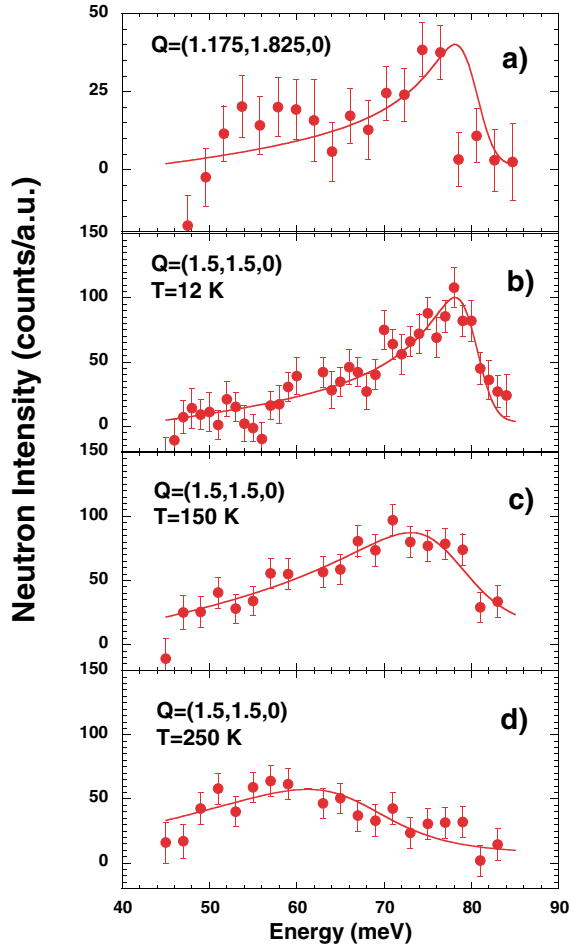


FIG. 3 (color online). Energy scans at (a)  $\mathbf{Q} = (1.175, 1.825, 0)$ , (b)–(d)  $\mathbf{Q} = (1.5, 1.5, 0) \equiv \mathbf{Q}_{\text{AF}}$ , after subtraction of background measured either at  $\mathbf{Q} = (1, 2, 0)$  or by rocking the sample by  $\pm 15^\circ$ . The data have been obtained with  $E_f = 41$  meV. The solid lines represent best fits of a damped harmonic oscillator function, with a dispersion relation as shown in Fig. 2(a), convolved with the spectrometer resolution. The line in (a) is the same as in (b) except for a scale factor.

stripe domains, and the magnetic form factor  $f(Q)$  is assumed to vary insignificantly across the range of a given scan. To fit the data, the model  $S(\mathbf{Q}, \omega)$  was convolved with the spectrometer resolution function, and the parameters  $Q_\omega$  and  $\Delta$  were varied to minimize  $\chi^2$ . The model provides reasonable fits to the data with a limited number of fitting parameters; note that the enhanced intensity near  $\mathbf{Q}_{\text{AF}}$  in Fig. 2(b) and 2(c) comes from the superposition of contributions dispersing from the four surrounding  $\mathbf{Q}_\delta$  points (see the upper panel of Fig. 1). The results obtained for  $Q_\omega$  as a function of energy transfer,  $\hbar\omega$ , are plotted in Fig. 2(a), together with  $\omega_0$  at  $H = 0.18, 0.5$ , and  $0.82$ . The momentum width,  $\Delta$ , when converted to half width at half maximum, is  $0.05 \text{ \AA}^{-1}$ .

To fit the constant- $\mathbf{Q}$  scans of Fig. 3, it is standard to use an alternative parametrization,

$$S(\mathbf{Q}, \omega) = A' f^2(Q) \frac{\omega \Gamma [1 + n(\omega, T)]}{[\omega^2 - \omega^2(\mathbf{Q})]^2 + \omega^2 \Gamma^2}, \quad (2)$$

where  $\omega(\mathbf{Q}) = \omega_0 - \alpha(\mathbf{Q} - \mathbf{Q}_{\text{AF}})^2$  ( $\alpha = 170 \text{ meV \AA}^2$ ), and  $n(\omega, T)$  is the Bose temperature factor. The temperature dependence of the parameters  $\omega_0$  and  $\Gamma$  are plotted in Fig. 4, while the low-temperature result for  $\omega_0$  is plotted in Fig. 2(a).

The spin-wave dispersion determined by the quantitative analysis can be described fairly well by a very simple expression,  $\omega(\mathbf{Q}) = \omega_0 |\sin(3\pi H)|$  along the  $[HH0]$  direction [22], indicated by the full line in Fig. 2(a). For comparison, the spin-excitation spectrum measured in undoped  $\text{La}_2\text{NiO}_4$  [23], shifted from  $\mathbf{Q}_{\text{AF}}$  to  $\mathbf{Q}_\delta$ , is indicated by dot-dashed lines. It matches the low-energy behavior surprisingly well, but clearly deviates at high energy. The  $\mathbf{Q}_{\text{AF}}$  crossing of the shifted curves is at 106 meV, while the measured  $\omega_0$  is renormalized down to 80 meV. Besides the maximum at  $H = \frac{1}{2}$ , the model dispersion curve also has maxima at  $H = \pm \frac{1}{6}$ . The energy scan at  $H \approx \frac{1}{6}$  shown in Fig. 3(a) is consistent with that at  $\mathbf{Q}_{\text{AF}}$ , Fig. 3(b), as expected for conventional spin waves. Looking at Fig. 2(a), one might expect to find an additional optical spin-wave branch at higher energies ( $\leq 125$  meV); searches at energies of up to 100 meV did not yield any positive evidence for such a branch.

It is interesting to compare the doping dependence of the maximum spin-excitation frequency,  $\omega_0$ , with that of the “2-magnon frequency,”  $\nu_{2\text{mag}}$ , determined by Raman scattering [24–26]. We find that the ratio  $\omega_0(x = 0.31)/\omega_0(x = 0) = 80 \text{ meV}/124 \text{ meV} = 0.65$  is very similar to  $\nu_{2\text{mag}}(x = 0.33)/\nu_{2\text{mag}}(x = 0) = 1110 \text{ cm}^{-1}/1640 \text{ cm}^{-1} = 0.68$ . In the Raman studies of the  $x = 0.33$  phase [24,25], a second, lower-energy peak at  $720 \text{ cm}^{-1}$  ( $\equiv 90 \text{ meV}$ ) was also attributed to 2-magnon scattering; however, we do not observe any features in the single-magnon dispersion that would

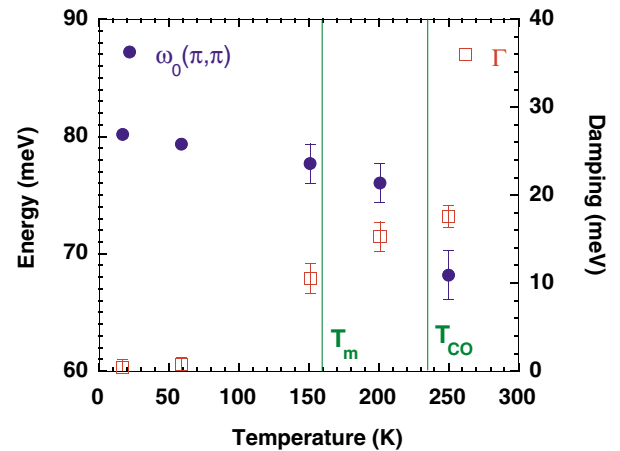


FIG. 4 (color online). Temperature dependence of various fitting parameters: Spin-wave energy maximum (left scale) and damping energy at  $\mathbf{Q}_{\text{AF}}$  (right scale). Vertical lines indicate the magnetic and charge-order transitions.

correlate with a second 2-magnon peak. Alternatively, Raman measurements on oxygen-doped  $\text{La}_2\text{NiO}_4$  [26] suggest that the  $720\text{ cm}^{-1}$  feature might be associated with a phonon mode, observed even in undoped  $\text{La}_2\text{NiO}_4$ , that should be Raman inactive.

To evaluate the anisotropy in the dispersion, we return to the 28-meV data of Fig. 1. By fitting the resolution-convolved Eq. (1) to the low-temperature data, we can estimate the spin-wave velocity,  $c_s = \omega/Q_\omega$ , along directions parallel and perpendicular to the stripes. Consistent with the figure, we find little anisotropy, with  $\hbar c_{s\parallel} = 300 \pm 20\text{ meV \AA}$  and  $\hbar c_{s\perp} = 350 \pm 20\text{ meV \AA}$ . Both of these values are close to the value of  $\hbar c_0 = 340\text{ meV \AA}$  obtained in pure  $\text{La}_2\text{NiO}_4$  [23]. Furthermore, the anisotropy in the spin-wave velocity between the directions parallel and perpendicular to the stripes is less than 15%. Such a lack of significant anisotropy is rather counter-intuitive. The observation of well-defined excitations following a simple dispersion curve such as shown in Fig. 2(a) is rather remarkable relative to the large hole concentration. One can suggest that charge order coherently affects the spin dynamics for this hole filling near  $\frac{1}{3}$  due to pinning effects.

As shown by Figs. 1 and 3, a striking temperature dependence is observed at energies much larger than  $kT$ . With increasing temperature, the magnetic mode at  $\mathbf{Q}_{\text{AF}}$  softens and broadens (Fig. 4). The frequency reduction and damping are of comparable magnitude. Even above the charge-ordering transition, the mode remains underdamped. This observation is consistent with the stripe-liquid phase proposed to describe the low-energy spin dynamics [19].

Returning to our original motivation, the spin-excitation spectrum in the stripe-ordered nickelate agrees with the proposed spin-only incommensurate model [17], especially the behavior observed around  $\mathbf{Q}_{\text{AF}}$ . Although this dispersion about  $\mathbf{Q}_{\text{AF}}$  is certainly similar to that measured in the superconducting state of  $\text{YBa}_2\text{Cu}_3\text{O}_{6.85}$  [5], there are also instructive differences: we observe excitations dispersing away from  $\mathbf{Q}_{\text{AF}}$  for which no parallel is found in the cuprate. While there is some enhancement of the intensity at  $\omega_0$  due to overlapping contributions from orthogonal stripe domains, it is modest compared to the resonant enhancement in the cuprate. Finally, the nickelate results provide no direct insight into the temperature dependence of the resonance peak in the superconductor. In particular, the rapid growth in intensity of the resonance peak below the superconducting transition is left unexplained. These deficiencies do not rule out a role for spatial inhomogeneity in the cuprates; however, a more realistic model would probably require inclusion of the interaction between the correlated spins and hole pairs.

In conclusion, we have measured the full spin-excitation spectrum perpendicular to the ordered stripes in the nickelate  $\text{La}_{1.69}\text{Sr}_{0.31}\text{NiO}_4$ . The spin dynamics is found to be surprisingly similar to a standard incommensurate

antiferromagnet with an almost isotropic spin-wave velocity. While intriguing in their own right, these results show that a spin-only approach provides an insufficient model for the magnetic resonance feature observed in several high- $T_c$  cuprates.

We thank A.V. Balatsky, C. Morais-Smith, and J. Zaanen for fruitful discussions. The work at Brookhaven is supported by U.S. Department of Energy Contract No. DE-AC02-98CH10886. The work at ISSP is supported by a Grant-In Aid for Scientific Research from the Ministry of Education, Culture, Sports, Science, and Technology, Japan.

*Note added.*—After submission, similar measurements were reported by Boothroyd *et al.* [27].

---

\*Present address: II. Physics Institute, Universitat zu Köln, Zùlpicher Strasse 77, D-50937 Köln, Germany.

- [1] H. He *et al.*, *Science* **295**, 1045 (2002).
- [2] P. Bourges, in *The Gap Symmetry and Fluctuations in High-Temperature Superconductors*, edited by J. Bok, G. Deutscher, D. Pavuna, and S. A. Wolf (Plenum, New York, 1998), p. 349.
- [3] H. A. Mook *et al.*, *Nature (London)* **395**, 580 (1998).
- [4] M. Arai *et al.*, *Phys. Rev. Lett.* **83**, 608 (1999).
- [5] P. Bourges *et al.*, *Science* **288**, 1234 (2000).
- [6] F. Onufrieva and P. Pfeuty, *Phys. Rev. B* **65**, 054515 (2002).
- [7] M. R. Norman, *Phys. Rev. B* **63**, 092509 (2001).
- [8] A. V. Chubukov, B. Jankó, and O. Tchernyshyov, *Phys. Rev. B* **63**, 180507R (2001).
- [9] J. Brinckmann and P. A. Lee, *Phys. Rev. B* **65**, 014502 (2002).
- [10] V. J. Emery, S. A. Kivelson, and J. M. Tranquada, *Proc. Natl. Acad. Sci. U.S.A.* **96**, 8814 (1999).
- [11] J. Zaanen, *Science* **286**, 251 (1999).
- [12] J. Zaanen, M. L. Horbach, and W. van Saarloos, *Phys. Rev. B* **53**, 8671 (1996).
- [13] N. Hasselmann *et al.*, *Phys. Rev. Lett.* **82**, 2135 (1999).
- [14] S. Sachdev, *Science* **288**, 475 (2000).
- [15] E. Kaneshita *et al.*, *J. Phys. Soc. Jpn.* **70**, 866 (2001).
- [16] S. Varlamov and G. Seibold, *Phys. Rev. B* **65**, 075109 (2002).
- [17] C. D. Batista, G. Ortiz, and A. V. Balatsky, *Phys. Rev. B* **64**, 172508 (2001).
- [18] J. M. Tranquada, P. Wochner, and D. J. Buttrey, *Phys. Rev. Lett.* **79**, 2133 (1997).
- [19] S.-H. Lee *et al.*, *Phys. Rev. Lett.* **88**, 126401 (2002).
- [20] H. Yoshizawa *et al.*, *Phys. Rev. B* **61**, R854 (2000).
- [21] J. M. Tranquada *et al.*, *Phys. Rev. Lett.* **88**, 075505 (2002).
- [22] This expression is identical to  $|\cos[\frac{\pi}{2\delta}(H - 0.5)]|$  with  $\delta = 1/6$  which corresponds to the expected spin-wave dispersion for an incommensurate antiferromagnet.
- [23] K. Nakajima *et al.*, *J. Phys. Soc. Jpn.* **62**, 4438 (1993).
- [24] G. Blumberg, M. V. Klein, and S.-W. Cheong, *Phys. Rev. Lett.* **80**, 564 (1998).
- [25] K. Yamamoto *et al.*, *Phys. Rev. Lett.* **80**, 1493 (1998).
- [26] S. Sugai *et al.*, *J. Phys. Soc. Jpn.* **67**, 2992 (1998).
- [27] A. Boothroyd *et al.*, cond-mat/0206536.